Proc. Natl. Acad. Sci. USA
Vol. 95, pp. 15382–15387, December 1998
Cell Biology

A transgenic mouse model of metastatic prostate cancer originating from neuroendocrine cells

(prostatic intraepithelial neoplasia)

EMILY M. GARABEDIAN*, PETER A. HUMPHREY†, AND JEFFREY I. GORDON*‡

Departments of *Molecular Biology and Pharmacology and †Pathology, Washington University School of Medicine, St. Louis, MO 63110

Communicated by David M. Kipnis, Washington University School of Medicine, St. Louis, MO, October 23, 1998 (received for review September 14, 1998)

ABSTRACT **A transgenic mouse model of metastatic prostate cancer has been developed that is 100% penetrant in multiple pedigrees. Nucleotides −6500 to +34 of the mouse cryptdin-2 gene were used to direct expression of simian virus 40 T antigen to a subset of neuroendocrine cells in all lobes of the FVB/N mouse prostate. Transgene expression is initiated between 7 and 8 weeks of age and leads to development of prostatic intraepithelial neoplasia within a week. Prostatic intraepithelial neoplasia progresses rapidly to local invasion. Metastases to lymph nodes, liver, lung, and bone are common by 6 months. Tumorigenesis is not dependent on androgens. This model indicates that the neuroendocrine cell lineage of the prostate is exquisitely sensitive to transformation and provides insights about the significance of neuroendocrine differentiation in human prostate cancer.**

Cancer of the prostate (CaP) is currently the second leading cause of cancer deaths in men (1). Diagnosis of CaP has become common because of the availability of a rapid and sensitive screening test for prostate-specific antigen (PSA, ref. 2). This has produced a dilemma: how to accurately stratify patients into risk categories for development of aggressive disease. This poor prognostic capability reflects, in part, our lack of understanding of the molecular mediators of tumor progression.

The prostate is a tubuloalveolar gland that contains a simple, slowly renewing epithelium composed of three cell types (3). Secretory (luminal) cells predominate. Basal cells are interposed between luminal cells and the basement membrane and form the principal proliferating epithelial population in mature glands (4, 5). Neuroendocrine cells are rare and scattered throughout acini and ducts (6, 7). Neuroendocrine cells secrete a variety of growth factors that may affect development and maintenance of this tissue (e.g., calcitonin, bombesin, and parathyroid hormone-related protein; refs. 8–10).

Conventional adenocarcinoma of the prostate often displays focal neuroendocrine differentiation (NED): estimates of the frequency of NED vary depending on the detection methods employed but have been reported to be as high as 100% (reviewed in ref. 6). Studies suggest that NED is associated with an unfavorable prognosis (11–13) and androgen-independent progression (11, 14, 15). Several factors may contribute to this association. Some workers have noted that cells next to foci of NED exhibit increased proliferation and augmented expression of the antiapoptotic regulator Bcl-2 (e.g., ref. 16; reviewed in ref. 7). In addition, neuroendocrine cells in humans do not contain detectable levels of the androgen receptor (17).

Experimental models to explore the role of neuroendocrine cells in CaP are not available. The majority of research on CaP has been conducted by using human tissue samples, human cell lines, and animal models of sporadic, naturally occurring disease. In the interest of producing a reliable and relevant animal model of human CaP, several groups have expressed simian virus 40 large tumor antigen (SV40 T-Ag) in the secretory cells of transgenic mouse prostates. Expression results in neoplastic transformation of a subset of these cells and progression to invasive cancer (18–22). We now have developed a new transgenic mouse model in which SV40 T-Ag is produced in members of the neuroendocrine cell lineage, resulting in metastatic CaP.

MATERIALS AND METHODS

Generation of Transgenic Mice and Maintenance of Animals. Transgenic mice containing SV40 T-Ag, or nucleotides +3 to +2150 of the human growth hormone (hGH) gene, under the control of nucleotides −6500 to +34 of the mouse cryptdin-2 gene (CR2) were generated on an FVB/N background as described (23). Pedigrees were maintained as heterozygotes by crosses to normal FVB/N littermates. Mice containing CR2-T-Ag and CR2-hGH transgenes were identified by PCR (23). All animals were housed in microisolater cages and fed a standard irradiated chow diet *ad libitum* (Pico Rodent Chow 20, Purina).

Immunohistochemistry. Specified pathogen-free transgenic animals and nontransgenic littermate controls were sacrificed at 6, 7, 8, 10, 12, 16, or 24 weeks of age. Some animals were given an i.p. injection of an aqueous solution of BrdUrd (120 mg/kg) and 5-fluoro-2′-deoxyuridine (12 mg/kg) 90 min before sacrifice. Other cohorts of mice were castrated at 28 days of age.

After sacrifice, all pelvic, abdominal, and thoracic organs were examined for signs of metastasis or other gross pathology. Tissues, including pelvic and abdominal lymph nodes, liver, lung, brain, and femur, were then fixed by immersion in 10% buffered formalin (Fisher Scientific) or fresh periodate/lysine/paraformaldehyde solution for 6 h or 45 min, respectively. Dorsal, ventral, anterior, and lateral lobes of the prostate were removed *en bloc*, weighed, and measured with calipers before fixation. After fixation, all tissues were washed in 70% ethanol overnight and embedded in paraffin.

Paraffin-embedded sections were deparaffinized, rehydrated, and microwaved in 10 mM sodium citrate buffer, pH 6.0. After antigen retrieval, slides were washed in distilled water, placed in PBS-blocking buffer (1% BSA/0.2% nonfat dry milk/0.3% Triton X-100 in PBS) for at least 20 min, and then incubated at 4°C overnight with one or more of the following primary antibodies: (*i*) goat anti-BrdUrd (final dilution in PBS-blocking buffer, 1:1,000; ref. 24); (*ii*) rabbit anti-SV40 T-Ag (1:2,000; a generous

Abbreviations: CaP, cancer of the prostate; SV40, simian virus 40; PSA, prostate-specific antigen; NED, neuroendocrine differentiation; T-Ag, large T antigen; hGH, human growth hormone; FITC, fluorescein isothiocyanate; Cy3, indocarbocyanine; PIN, prostatic intraepithelial neoplasia; CR2, cryptdin-2 gene.

‡To whom reprint requests should be addressed at: Department of Molecular Biology and Pharmacology, Box 8103, Washington University School of Medicine, South Euclid Avenue, St. Louis, MO 63110. e-mail: jgordon@pharmsun.wustl.edu.

The publication costs of this article were defrayed in part by page charge payment. This article must therefore be hereby marked "*advertisement*" in accordance with 18 U.S.C. §1734 solely to indicate this fact.

gift of Doug Hanahan, University of California, San Francisco); (*iii*) rabbit anti-human synaptophysin (1:200; Dako); (*iv*) rabbit anti-bovine SP-1 chromogranin A (1:500; Incstar, Stillwater, MN); (*v*) sheep anti-human growth hormone (1:2,000; Cortex Biochem, San Leandro, CA); (*vi*) mouse anti-human high molecular weight cytokeratin (1:200; clone 34βE12; Dako); and (*vii*) rabbit anti-human androgen receptor (1:100; N20 from Santa Cruz Biotechnology; recognizes an epitope at the N terminus of the orthologous human and mouse proteins).

Antigen–antibody complexes were detected with fluorescein isothiocyanate (FITC)-, indocarbocyanine (Cy3)-, or indodicarbocyanine-conjugated donkey anti-rabbit or anti-goat IgG (diluted 1:200 and 1:500, respectively; Jackson ImmunoResearch). Mouse anti-high molecular weight cytokeratin was detected by using the tyramide signal amplification direct FITC kit (NEN). Slides were counterstained with bis-benzimide (Sigma) and viewed and photographed with a Zeiss Axioscope or a Molecular Dynamics Multiprobe 2001 inverted confocal microscope (1-μm section scans). Alternatively, bound primary rabbit antibodies were visualized with horseradish peroxidase-conjugated donkey anti-rabbit IgG (1:100; Jackson ImmunoResearch) and 3,3′-diaminobenzidine/metal substrate (Pierce).

Morphometric Studies. Prostates fixed in 10% formalin and embedded in paraffin were serially sectioned (5 μm) in their entirety. Every 10th section was stained with hematoxylin and eosin and evaluated by light microscopy for the presence of high-grade prostatic intraepithelial neoplasia (PIN) and invasive carcinoma. The extent of high-grade PIN was quantitated by recording the number of separate foci of PIN (25) per section. The size of carcinomas was determined with an ocular micrometer (microscopic tumors) or calipers (macroscopically evident tumors). Tumor volume (cm^3) was calculated by using the formula for spheres.

RESULTS

CR2-T-Ag Transgenic Mice Develop CaP with a Pattern of Progression That Resembles Human Prostate Cancer. FVB/N transgenic mice expressing SV40 T-Ag under the control of nucleotides −6500 to +34 of the mouse CR2 gene originally were created to study the function of Paneth cells, one of the four epithelial lineages in the small intestine (23). Paneth cells secrete growth factors and antimicrobial peptides (cryptdins) (26). Mature Paneth cells are absent in CR2-T-Ag mice because SV40 T-Ag blocks their terminal differentiation and induces cell death. Their absence produces no discernible effect on overall intestinal physiology or mucosal barrier function and does not lead to development of intestinal neoplasms (23).

CR2 is undetectable in the prostate of normal adult FVB/N mice, as defined by reverse transcriptase–PCR (RT-PCR) or immunohistochemistry (data not shown). CR2 promoter-directed expression of SV40 T-Ag in the prostate first came to our attention when male CR2-T-Ag transgenic mice belonging to four different pedigrees died at 5–7 months of age with large prostate tumors. Prostate cancer was observed in 100% of male transgenics from these pedigrees (n = 77 animals surveyed at 5–6 months). Two pedigrees were expanded for further analysis. Both lines of mice displayed 100% penetrance and similar histopathologic and temporal patterns of progression of their CaP.

Transgenic animals and their normal (nontransgenic) littermates were sacrificed at 7, 8, 10, 12, 16, and 24 weeks of age, and their prostates were subjected to morphometric analysis (n = 6–21 mice/genotype/time point). No abnormalities were seen in the prostates of any normal controls (n = 44; e.g., Fig. 1*A*).

The earliest histologic abnormalities in transgenic mice were detected at 8 weeks of age. This coincides with the initiation of SV40 T-Ag expression in the prostatic epithelium (see below). At 8 and 10 weeks, all glands had scattered foci of increased cellularity with multiple mitotic and apoptotic figures (Table 1 and Fig. 1*B*). Cells in these foci had enlarged nuclei of variable size and shape, increased chromatin density and clumping, multiple enlarged nucleoli, as well as attenuation of cytoplasmic volume and features (Fig. 1*C*). These foci resemble PIN, postulated to be a precursor to CaP in humans (27). The average frequency of PIN at 8 and 10 weeks was 1.3 and 2.8 foci per 5-μm-thick section of prostate (Fig. 2).

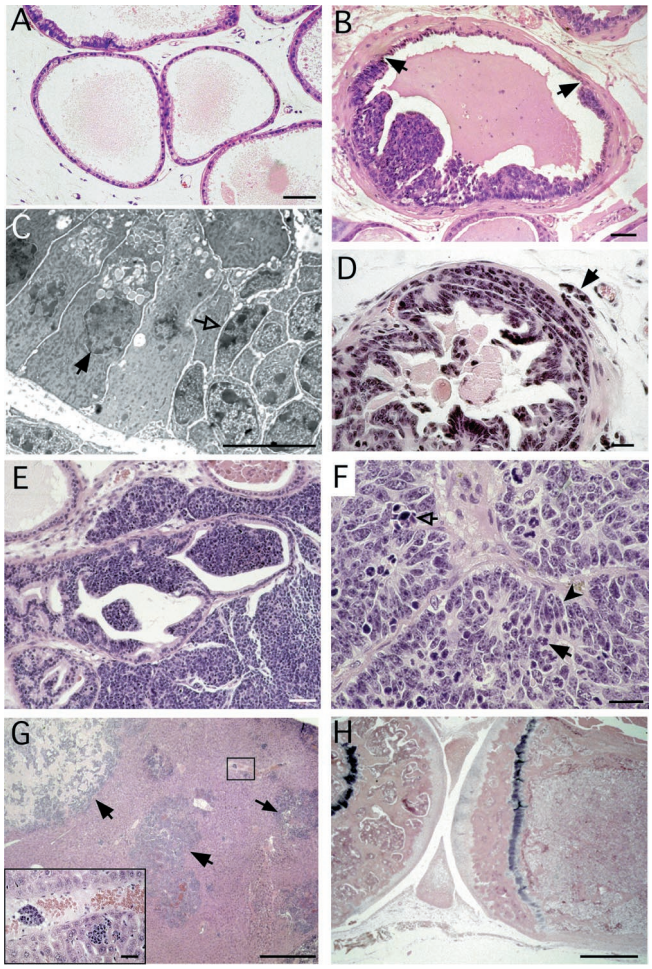

FIG. 1. Progression of lesions in CR2-T-Ag mouse prostates recapitulates the proposed histologic progression of human prostate cancer. (*A*) Hematoxylin- and eosin-stained section from a nontransgenic 8-week-old mouse, demonstrating the appearance of normal prostatic epithelium. (*B*) Prostatic intraepithelial neoplasia (PIN) in an 8-week-old CR2-T-Ag mouse. Borders between normal-appearing epithelium and clusters of dysplastic cells contained in foci of PIN are indicated by arrows. (*C*) Transmission electron microscopy of a border, such as that shown in *B*. In contrast to normal nuclei (e.g., closed arrow), dysplastic nuclei (e.g., open arrow) have irregular size and shape, clumps of condensed chromatin, and multiple nucleoli. (*D*) By 12 weeks of age, invasion through the basement membrane into the surrounding stroma has begun (e.g., arrow). (*E*) At 16 weeks, stromal invasion is extensive, with glandular structures being replaced by tumor. (*F*) A 24-week-old transgenic mouse prostate consisting of sheets of neoplastic cells. High rates of mitosis (solid arrow) and apoptosis (open arrow) are evident. Spindle-shaped cells (e.g., solid arrowhead) are consistent with neuroendocrine differentiation. (*G*) Liver from a 24-week-old animal with evidence of metastases (e.g., arrows). *Inset* is a high-power view of the boxed region showing hematogenous spread of the cancer. (*H*) At 24 weeks, the femoral marrow space is filled with tumor cells. The tibia (located on the left) is included to show the appearance of unaffected marrow. [Bars = 50 μm (*A*, *B*, and *E*); 10 μm (*C*); 20 μm (*D* and *F*); 500 μm (*G* and *H*).]

By 12 weeks of age, all transgenic prostates contained multifocal PIN (Table 1 and Fig. 2). In 70% of mice surveyed, local invasion of neoplastic cells through the basement membrane and into the surrounding stroma was observed (Fig. 1*D*) These

Table 1. Temporal pattern of progression of prostate cancer in CR2-T-Ag transgenic mice

Age of sacrifice	PIN	Local invasion	Grossly evident nodules (≥3 mm)	Lymphatic or vascular invasion or micrometastases in liver	Grossly evident metastases
7 weeks	0/6	0/6	0/6	0/6	0/6
8 weeks	6/6	0/6	0/6	0/6	0/6
10 weeks	17/18	1/18	0/18	0/18	0/18
12 weeks	7/7	5/7	0/7	0/7	0/7
16 weeks	12/12	11/12	3/12	3/12	1/12
24 weeks	21/21	21/21	21/21	18/21	8/21

observations support the hypothesis that PIN represents a precursor to cancer.

At 16 weeks, 90% of transgenic prostates had invasion of cells through the basement membrane into the surrounding stroma (Fig. 2). Frequently, a single section would contain multiple neoplastic lesions at different stages of evolution. Twenty-five percent of animals surveyed had prostatic nodules ≥3 mm in diameter that were composed of sheets of malignant cells with little or no glandular features (Fig. 1*E*). Examples of vascular, lymphatic, and perineural invasion also were found within these glands (Table 1).

By 24 weeks, 100% of prostates contained large tumor nodules composed of solid masses of neoplastic cells (Fig. 1*F*). At this age, adenocarcinomas in 40% of CR2-T-Ag males surveyed had metastasized to abdominal lymph nodes, liver, lung, and bone marrow (Table 1, Fig. 1 *G* and *H*).

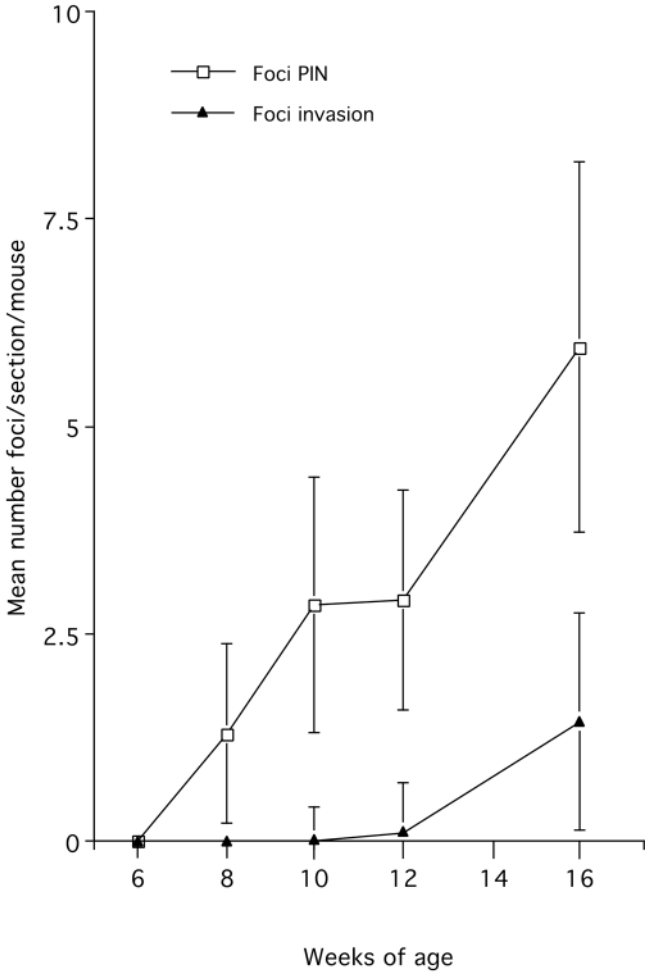

FIG. 2. Morphometric analysis of the number of foci of PIN and invasion in the prostates of 7- to 16-week-old CR2-T-Ag mice. Mean values ± SE are shown.

Male mice from both pedigrees of mice typically died between 5 and 7 months of age. In contrast, CR2-T-Ag females ($n = 50$) developed normally and had a normal lifespan when compared with their nontransgenic female (or male) littermates.

Studies of CR2-T-Ag, CR2-hGH, and Bitransgenic Mice Establish that Neuroendocrine Cells Are Very Sensitive to Transformation by SV40 T-Ag. Hematoxylin- and eosin-stained sections of the prostate tumors revealed a number of features suggestive of neuroendocrine differentiation, e.g., spindle-shaped cells and occasional rosette-like structures (Fig. 1*F*). This raised the question of whether CaP in these mice was initiated in members of the neuroendocrine cell lineage.

At 6 and 7 weeks of age, transgene expression was undetectable by RT-PCR or Western blot assays or by immunohistochemical analysis of prostates that had been serially sectioned in their entirety ($n = 6$ mice/time point; data not shown). One week later, SV40 T-Ag was present in six of six serially sectioned transgenic prostates and confined to epithelial cells located in foci of PIN (Fig. 3*A*). These SV40 T-Ag-expressing cells invariably stained positive for two neuroendocrine markers—synaptophysin and chromogranin A (Fig. 3*B*). They were found only in clusters (i.e., never as single, isolated cells), and they never had normal morphology. Multilabel immunohistochemical surveys of prostates obtained from mice given an i.p. injection of 5-bromo-2′-deoxyuridine 90 min before sacrifice established that the dysplastic, SV40 T-Ag-positive neuroendocrine cells were actively proliferating (Fig. 3*C*).

In 8-week-old mice, these neuroendocrine cells typically were located between the basement membrane and an overlying layer of SV40 T-Ag-negative secretory cells with normal morphology. In foci of more advanced PIN, SV40 T-Ag-positive neuroendocrine cells appeared to "erupt" through this layer of normal secretory cells, producing cellular tufts that protrude into the lumen of acini. As animals aged, coexpression of SV40 T-Ag and these neuroendocrine markers was maintained, even as cells invaded surrounding stroma, and metastasized to regional lymph nodes. Electron microscopy studies of prostate tumors and of organ metastases from 24-week-old mice revealed neuroendocrine granules (data not shown).

These results indicate that tumorigenesis is fully penetrant in several pedigrees of FVB/N CR2-T-Ag mice and is initiated in a neuroendocrine cell population that is exquisitely sensitive to neoplastic transformation. The latter conclusion is based on the observation that dysplasia is manifest in all cells that express the transgene from the very first time that the viral oncoprotein becomes detectable.

To further validate this proposed pathogenetic scheme, and to test whether nucleotides −6400 to +34 of the mouse CR2 gene are sufficient to restrict expression of other foreign gene products to neuroendocrine cells, we analyzed the cellular patterns of expression of another, more neutral reporter, hGH, in three pedigrees of FVB/N CR2-hGH mice. At 12 weeks of age, hGH was detectable in a small number (<0.3%) of scattered cells in the prostatic epithelium. The hGH-producing cells had prominent cytoplasmic processes that contacted neighboring epithelial cells (Fig. 4*A*). These processes are a known morphologic feature of

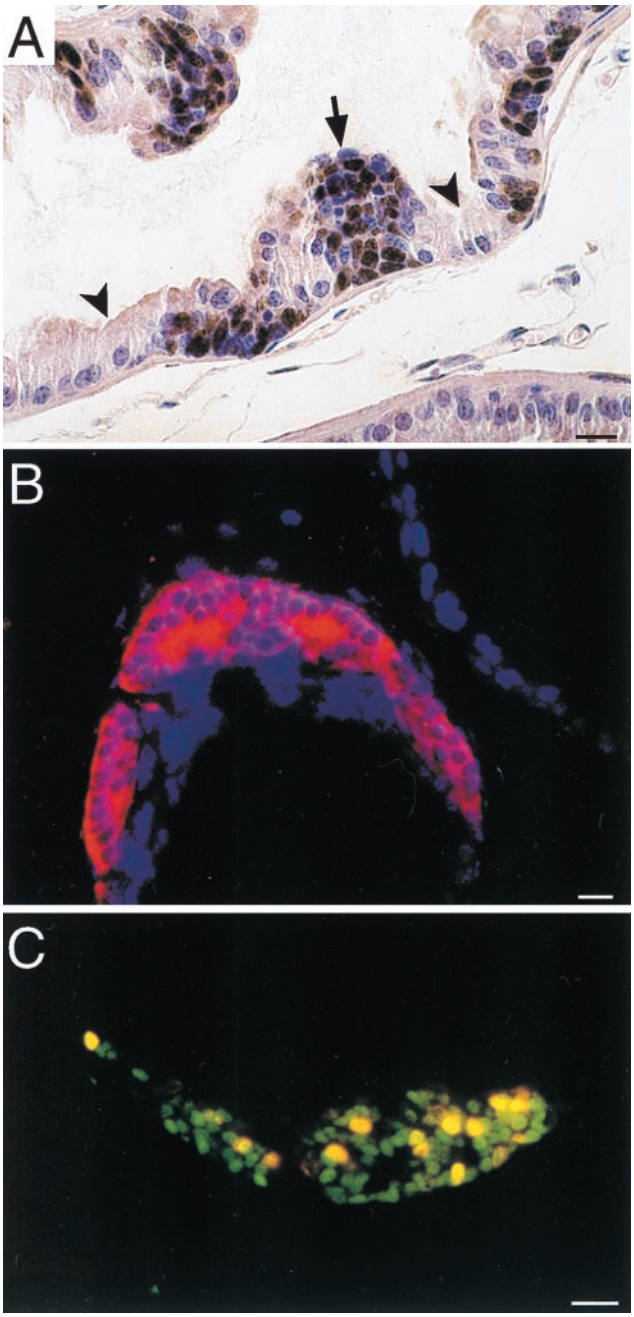

FIG. 3. Foci of PIN are composed of SV40 T-Ag-expressing neuroendocrine cells. (*A*) Section from an 8-week-old CR2-T-Ag mouse prostate stained with rabbit anti-SV40 T-Ag, horseradish peroxidase-conjugated donkey anti-rabbit IgG, and diaminobenzidine, then counterstained with hematoxylin and eosin. SV40 T-Ag appears brown. The arrow points to a cluster of SV40 T-Ag-positive cells, whose morphology is distinct from their normal, SV40 T-Ag-negative epithelial neighbors (e.g., arrowheads). (*B*) Section from an 8-week-old CR2-T-Ag mouse showing a focus of PIN containing amplified neuroendocrine cells. The section was stained with rabbit anti-synaptophysin and Cy3-donkey anti-rabbit IgG. (*C*) Section from the prostate of an 8-week-old CR2-T-Ag transgenic mouse that received an injection of BrdUrd 90 min before sacrifice. The section was incubated with goat anti-BrdUrd (detected with Cy3-donkey anti-goat IgG) and rabbit anti-SV40 T-Ag (detected with FITC-donkey anti-rabbit IgG). Proliferating epithelial cells (yellow nuclei) are restricted to the cluster of SV40 T-Ag-positive cells. (Bars = 20 μm.)

neuroendocrine cells (28). Multilabel immunohistochemistry and confocal microscopy demonstrated coexpression of hGH and synaptophysin or chromogranin A as well as the absence of high

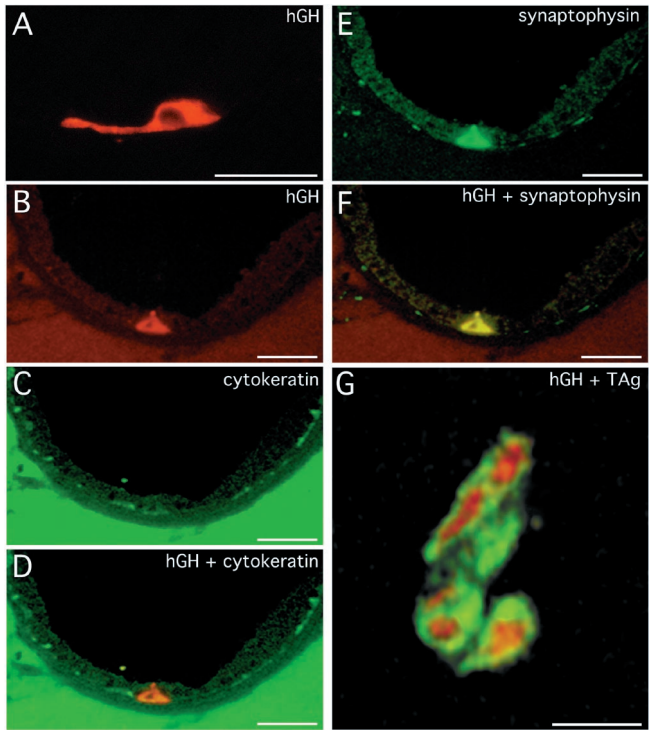

FIG. 4. Evidence that prostate cancer is initiated in a subset of neuroendocrine cells where nucleotides −6400 to +34 of the mouse cryptdin gene are active. (*A*) hGH-positive cell with prominent cytoplastic processes, in the prostate of a 12-week-old CR2-hGH transgenic mouse. The section was stained with sheep anti-hGH and Cy3-donkey anti-sheep IgG. (*B–F*) Multilabel confocal photomicrographs, taken in the same 1-μm-thick focal plane, of a prostate section from a 12-week-old CR2-hGH animal. The section was stained with sheep anti-hGH (detected with Cy3-donkey anti-sheep IgG), mouse anti-high molecular weight cytokeratin (detected with horseradish peroxidase-donkey anti-mouse IgG and FITC-tyramide), and rabbit antisynaptophysin (detected with indodicarbocyanine-donkey anti-rabbit IgG). (*B*) A single wedge-shaped hGH-positive cell is detected as red. (*C*) When cytokeratin is visualized (green), this cell is not evident. (*D*) Combined images from *A* and *B* show that the hGH-positive cell does not express cytokeratin, indicating that it does not belong to the basal cell lineage. (*E*) Indodicarbocyanine is assigned a green color to show synaptophysin immunoreactivity. (*F*) Combining the images shown in *B* and *E* reveals that the hGH-positive cell coexpresses synaptophysin, i.e., it is a member of the neuroendocrine lineage. (*G*) Conventional light microscopy of a 5-μm-thick section prepared from a 12-week-old bitransgenic mouse containing both CR2-hGH and CR2-T-Ag. The section was stained with sheep anti-hGH (detected with FITC-donkey anti-sheep IgG) and rabbit anti-SV40 T-Ag (detected with Cy3-donkey anti-rabbit IgG). Cells in a focus of PIN coexpress SV40 T-Ag (red-orange nuclei) and hGH (green cytoplasm). (Bars = 20 μm.)

molecular weight cytokeratin, a marker of basal cells (29) (Fig. 4 *B–F*).

Multilabel immunohistochemistry indicated that not all synaptophysin or chromogranin A immunoreactive cells in the prostates of CR2-hGH mice were hGH-positive. Serial sectioning of the prostate in its entirety established that the CR2 promoter is active in a subset of neuroendocrine cells located in the proximal ducts and distal acini of all lobes of the prostate, including the coagulating glands (n = 4 animals). hGH was not detectable in intestinal enteroendocrine cells or in any part of the female urogenital system of CR2-hGH mice (n = 3; data not shown).

FVB/N CR2-hGH transgenics subsequently were crossed to FVB/N CR2-T-Ag mice to generate bitransgenic animals. At 12 weeks of age, multilabel immunohistochemical surveys of the serially sectioned prostate revealed that hGH-positive cells in

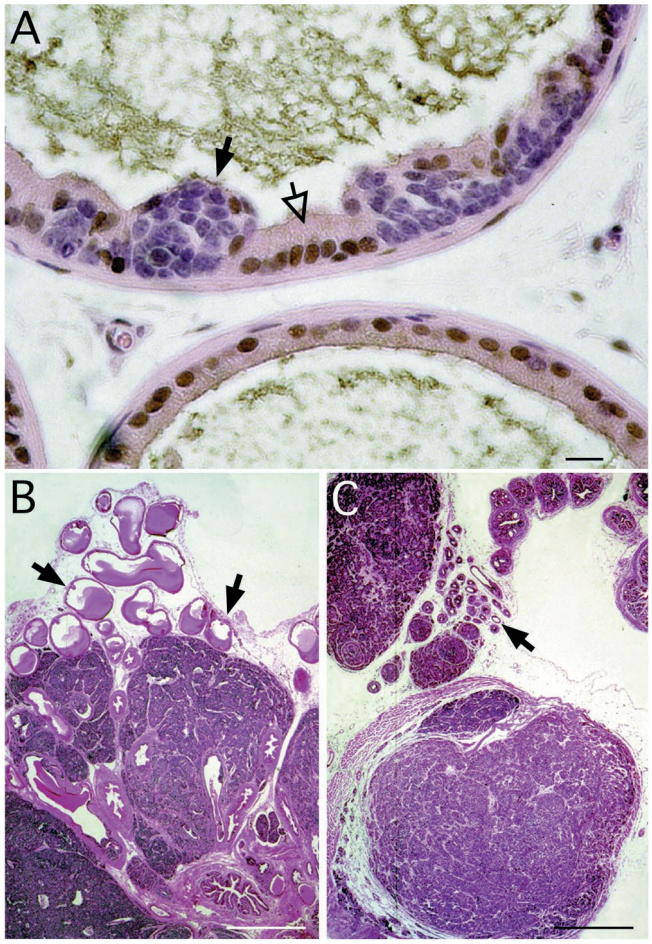

FIG. 5. Castration does not affect the growth of prostate cancers in CR2-T-Ag mice. (*A*) Section from a 10-week-old CR2-T-Ag prostate was stained with rabbit anti-androgen receptor, horseradish peroxidase-donkey anti-rabbit IgG, and diaminobenzidine, and then counterstained with hematoxylin and eosin. Immunoreactive androgen receptor (brown) is located in the normal glandular epithelium (e.g., open arrows) and stroma, but not in cells contained within a focus of PIN (e.g., solid arrow). (*B*) Hematoxylin- and eosin-stained section of prostate from a noncastrated 16-week-old CR2-T-Ag mouse. Arrows point to normal glandular epithelium. (*C*) Section from a CR2-T-Ag mouse castrated at 4 weeks and then sacrificed at 16 weeks of age. Comparison with *B* reveals that while the nonneoplastic epithelium has undergone atrophy (arrow), the histopathologic features of neoplastic foci are unaffected by castration. [Bars = 20 μm (*A*) and 500 μm (*B* and *C*).]

areas of PIN coexpressed SV40 T-Ag and that all SV40 T-Ag-positive cells produced hGH (e.g., Fig. 4*G*). These findings confirm that the CR2-transcriptional regulatory elements are active only in a subset of prostatic neuroendocrine cells and that SV40 T-Ag expression in this population is sufficient to initiate tumorigenesis.

CR2-T-Ag Prostate Tumors Are Not Sensitive to Androgens. As noted in the Introduction, neuroendocrine cells in humans lack detectable levels of the androgen receptor and neuroendocrine differentiation in human CaP is associated with androgen-independent growth. We used our CR2-T-Ag transgenic mouse model to explore whether androgens are required for initiation and/or progression of a neuroendocrine cell-derived CaP.

Mice from each pedigree were sacrificed at 8–24 weeks of age, and androgen receptor expression in their prostates was defined by using immunohistochemistry. In 8-week-old CR2-T-Ag animals, androgen receptor is detectable in stromal and normal secretory epithelial cells but not in SV40 T-Ag-positive neuroendocrine cells present in foci of early PIN (Fig. 5*A*). Analysis of 10- and 24-week-old mice established that neoplastic cells remain androgen receptor-negative during subsequent progression.

Transgenic mice were castrated at 4 weeks of age and then sacrificed at 10, 16, or 24 weeks of age (n = 12 mice per time point). At 10 weeks, castration produced a statistically significant reduction in both the weight and volume of the prostate. However, morphometric studies revealed that this was because of atrophy of normal glandular tissue: the number of foci of PIN and the histopathologic character of the lesions were indistinguishable from those of age-matched, noncastrated CR2-T-Ag controls. By 16 and 24 weeks of age, the weight and volume of tumors from castrated CR2-T-Ag animals were not significantly different ($P > 0.05$) from those of age-matched, noncastrated transgenic littermates (e.g., Fig. 5 *B* and *C*). These findings indicate that progression of CaP produced by SV40 T-Ag production in mouse neuroendocrine cells does not require androgens.

DISCUSSION

The occurrence of neuroendocrine differentiation in human prostate cancer is well documented, but not well understood. Explanations for the presence of neuroendocrine cells in adenocarcinoma of the human prostate include: (*i*) entrapment of normal neuroendocrine cells in an expanding tumor; (*ii*) proliferation of nontransformed neuroendocrine cells in response to paracrine factors released by neoplastic cells derived from another lineage; (*iii*) tumorigenesis is multifocal and initiation occurs in the neuroendocrine as well as other cell lineages; or (*iv*) initiation of tumorigenesis occurs in a multipotent stem cell that can give rise to neuroendocrine and secretory cell lineages. Although evidence supporting any one of these explanations is scarce, most investigators favor the last explanation (30).

Much of the uncertainty about the pathogenetic significance of NED derives from a lack of knowledge of neuroendocrine cell biology. These cells are rare in the normal human prostatic epithelium (28, 31) and even rarer in the mouse prostate. There is no reported cell line that fully recapitulates a differentiated prostate neuroendocrine phenotype. The normal contributions of members of this lineage in the development and maintenance of prostatic epithelial and stromal cell populations are unknown. Moreover, their susceptibility to malignant transformation and role in promoting progression of tumorigenesis are untested. We now have developed a transgenic mouse model of rapidly evolving prostate cancer that is initiated in neuroendocrine cells. This model establishes that neuroendocrine cells are extremely sensitive to transformation, that initiation of tumorigenesis in this lineage recapitulates many of the histopathologic features of human CaP, and that the neuroendocrine-derived prostate cancer is not dependent on androgens for its evolution.

The exquisite sensitivity of neuroendocrine cells to transformation is underscored by our finding that initiation of SV40 T-Ag expression coincides with immediate development of a dysplastic cellular phenotype and progression to PIN over the course of just 1–2 weeks in all lobes of the mouse prostate. This response is quite different from the response of secretory cells to SV40 T-Ag. Several different promoters have been used to express the viral oncoprotein in these cells (18–22). In the transgenic adenocarcinoma mouse prostate (TRAMP) model, the rat probasin gene promoter was used to restrict expression of SV40 T-Ag to secretory cells in the dorsal and lateral lobes of the prostate (18, 19). In this and the other transgenic models, the onset of neoplasia is delayed as much as several months after transgene expression begins. Moreover, only a subset of SV40 T-Ag-positive secretory cells is transformed.

The rapid, stereotyped progression from PIN to locally invasive cancer observed in several pedigrees of FVB/N CR2-T-Ag mice strongly supports the notion that PIN is a precursor to prostate cancer. Early lesions in CR2-T-Ag prostates resemble typical tufted, micropapillary, and flat patterns of PIN seen humans,

raising the possibility that some human prostate cancers may also originate in the neuroendocrine cell.

Our morphometric analysis revealed that the number of foci of PIN per section of CR2-T-Ag prostate increases over time. Since studies of CR2-hGH mice established that CR2 transcriptional regulatory elements are activated in scattered neuroendocrine cells, it is not surprising that early PIN is multifocal. However, the subsequent increase in the number of foci of PIN per section should not be considered as proof that the number of initiation events increases with time: expansion of PIN from a fixed number of sites of initiation would increase the number of locations in which PIN is encountered per section of this tubuloalveolar gland.

In older CR2-T-Ag mice, there are multiple lesions at various stages of progression in the same section. Since invasion appears to develop exclusively from PIN, this finding could indicate that neoplasia is initiated at multiple sites during a limited period of time, and only some sites of PIN undergo progression. Alternatively, neoplasia may be initiated at multiple sites continuously throughout adulthood, and the probability of progression is equivalent at each site so that the areas of PIN adjacent to more advanced disease represent more recent sites of initiation. Since the onset of transgene expression in neuroendocrine cells at 8 weeks of age is associated with their very rapid transformation, we assume that for new sites of initiation to occur at subsequent ages, new populations of neuroendocrine cells must be generated that support transgene expression, or preexisting subpopulations must acquire the ability to support production of SV40 T-Ag.

In 35% of TRAMP mice, castration prevents tumorigenesis entirely (32). In the remaining 65%, androgen-independent growth of their secretory cell-derived tumors occurs after castration. These tumors have been characterized as being more frequently metastatic and less differentiated than tumors in noncastrated, age-matched transgenics, suggesting that androgen ablation therapy results in selection of more malignant tumors (32). In contrast, rapid progression to metastatic disease in the presence or absence of androgens is a notable feature of CaP in CR2-T-Ag mice. Our castration studies indicate that their neuroendocrine-derived tumors are either capable of rapidly becoming androgen-independent or are derived from a preexisting, androgen-independent cell population. The lack of detectable androgen receptor in neuroendocrine-derived foci of PIN supports the latter possibility. Our castration results also suggest that neuroendocrine cells are unresponsive to signals that may be derived from neighboring androgen receptor-positive stromal (or epithelial) cells.

Bonkhoff *et al.* (17) reported that neuroendocrine cells in humans do not contain detectable levels of androgen receptor. A number of workers have noted that NED is more extensive in androgen-independent human CaP. These observations suggest that human neuroendocrine cells (like mouse neuroendocrine cells) do not require androgens for their growth or survival, and therefore their fractional representation in CaP increases in response to the selective pressure of androgen ablation therapy (reviewed in ref. 3). Alternatively, the number of neuroendocrine cells may not change in response to androgen ablation therapy; rather, tumors with more NED may exhibit androgen-independent growth because their cellular populations manifesting NED are able to elaborate paracrine factors that influence the androgen responsiveness of neighboring populations of neoplastic cells without NED.

In summary, FVB/N CR2-T-Ag mice provide a model of a neuroendocrine cancer whose progression can be followed from the earliest stages of initiation to advanced metastatic disease. These animals offer an opportunity to recover the normally rare neuroendocrine cell, to study its biology, and to identify gene products whose expression or silencing contributes to initiation and/or progression of CaP. Some of these gene products also may be useful molecular markers for identifying individuals with a positive PSA who are at risk for, or are already developing, more aggressive disease. The highly reproducible and rapid evolution of CaP in these mice also makes them suitable for conducting crosses to other inbred strains to identify possible modifiers of their CaP, for genetic tests of the contribution of specified proteins to tumorigenesis, and for pharmacologic studies of potential therapeutic agents.

We thank Lisa Roberts, Sabrina Wagoner, Maria Karlsson, David O'Donnell, Paul Swanson, Kevin Roth, Elvie Taylor, Marlene Green, and Bill Coleman for their invaluable assistance. This work was supported by grants from the National Institutes of Health and Glaxo–Wellcome and is dedicated to Paul Garabedian and James Scarlett.

1. Parker, S. L., Tong, T., Bolden, S. & Wingo, P. A. (1996) *Ca Cancer J. Clin.* **46,** 5–27.
2. Schwartz, K. L., Severson, R. K., Gurney, J. G. & Montie, J. E. (1996) *Cancer* **78,** 1260–1266.
3. Bonkhoff, H. & Remberger, K. (1996) *Prostate* **28,** 98–106.
4. Bonkhoff, H., Stein, U. & Remberger, K. (1994) *Hum. Pathol.* **25,** 42–46.
5. Bonkhoff, H., Stein, U. & Remberger, K. (1994) *Prostate* **24,** 114–118.
6. di Sant'Agnese, P. A. (1992) *Hum. Pathol.* **23,** 287–296.
7. di Sant'Agnese, P. A. & Cockett, A. T. K. (1996) *Cancer* **78,** 357–361.
8. Bologna, M., Festuccia, C., Muzi, P., Biordi, L. & Ciomeni, M. (1989) *Cancer* **63,** 1714–1720.
9. Iwamura, M., Abrahamsson, P. A., Foss, K. A., Wu, G., Cockett, A. T. & Deftos L. J. (1994) *Urology* **43,** 675–679.
10. Shah, G., Rayford, W., Noble, M. J., Austenfeld, M., Weigel, J., Vamos, S. & Mebust, W. K. (1994) *Endocrinology* **134,** 596–602.
11. Abrahamsson, P. A., Falkmer, S., Falt, K. & Grimelius, L. (1989) *Pathol. Res. Pract.* **185,** 373–380.
12. Cohen, R. J., Glezerson, G. & Haffejee, Z. (1991) *Br. J. Urol.* **68,** 258–262.
13. Tetu, B., Ro, J. Y., Ayala, A. G., Johnson, D. E., Logothetis, C. J. & Ordonez, N. G. (1987) *Cancer* **59,** 1803–1809.
14. Kadmon, D., Thompson, T. C., Lynch, G. R. & Scardino, P. T. (1991) *J. Urol.* **146,** 358–361.
15. Logothetis, C. J. & Hoosein, N. M. (1996) in *Comprehensive Textbook of Genitourinary Oncology*, ed. Vogelzang, N. (Williams & Wilkins, Baltimore).
16. Segal, N. H., Cohen, R. J., Haffejee, Z. & Savage, N. (1994) *Arch. Pathol. Lab. Med.* **118,** 616–618.
17. Bonkhoff, H., Stein, U. & Remberger, K. (1993) *Virchows Arch. A Pathol. Anat.* **423,** 291–294.
18. Greenberg, N. M., DeMayo, F., Finegold, M. J., Medina, D., Tilley, W. D., Aspinall, J. O., Cunha, G. R., Donjacour, A. A., Matusik, R. J. & Rosen, J. M. (1995) *Proc. Natl. Acad. Sci. USA* **92,** 3439–3443.
19. Gingrich, J. R., Barrios, R. J., Morton, R. A., Boyce, B. F., DeMayo, F. J., Finegold, M. J., Angelopoulou, R., Rosen, J. M. & Greenberg, N. M. (1996) *Cancer Res.* **56,** 4096–4102.
20. Maroulakou, I. G., Anver, M., Garrett, L. & Green, J. E. (1994) *Proc. Natl. Acad. Sci. USA* **91,** 11236–11240.
21. Shibata, M.-A., Ward, J. M., Devor, D. E., Liu, M.-L. & Green, J. E. (1996) *Cancer Res.* **56,** 4894–4903.
22. Perez-Stable, C., Altman, N. H., Brown, J., Harbison, M., Cray, C. & Roos, B. A. (1996) *Lab Invest.* **74,** 363–373.
23. Garabedian, E. M., Roberts, L. J., McNevin, M. S. & Gordon, J. I. (1997) *J. Biol. Chem.* **272,** 23729–23740.
24. Cohn, S. M. & Lieberman, M. W. (1984) *J. Biol. Chem.* **259,** 12456–12462.
25. McNeal, J. E. & Bostwick, D. G. (1986) *Hum. Pathol.* **17,** 64–71.
26. Ouellette, A. J. & Selsted, M. E. (1996) *FASEB J.* **10,** 1280–1289.
27. Bostwick, D. G. (1995) *Cancer* **75,** 1823–1836.
28. Cohen, R. J., Glezerson, G., Taylor, L. F., Grundle, H. A. J. & Naudé, J. H. (1993) *J. Urol.* **150,** 365–368.
29. Bonkhoff, H. (1996) *Eur. Urol.* **30,** 201–205.
30. Bonkhoff, H., Stein, U. & Remberger, K. (1995) *Hum. Pathol.* **26,** 167–170.
31. Angelsen, A., Mecsei, R., Sandvik, A. K. & Wuldum, H. L. (1997) *Prostate* **33,** 18–25.
32. Gingrich, J. R., Barrios, R. J., Kattan, M. W., Nahm, H. S., Finegold, M. J. & Greenberg, N. M. (1997) *Cancer Res.* **57,** 4687–4691.